

## Heat-Induced Transformation of Nanodiamond into a Tube-Shaped Fullerene: A Molecular Dynamics Simulation

Gun-Do Lee,<sup>1</sup> C. Z. Wang,<sup>2</sup> Jaejun Yu,<sup>3</sup> Euijoon Yoon,<sup>1</sup> and K. M. Ho<sup>2</sup>

<sup>1</sup>*School of Materials Science and Engineering and Inter-university Semiconductor Research Center (ISRC), Seoul National University, Seoul 151-742, Korea*

<sup>2</sup>*Ames Laboratory and Department of Physics and Astronomy, Iowa State University, Ames, Iowa 50011, USA*

<sup>3</sup>*CSCMR and School of Physics, Seoul National University, Seoul 151-747, Korea*

(Received 21 July 2003; published 23 December 2003)

Heat-induced structural transformation in nanodiamond of diameter  $\sim 1.4$  nm is investigated by tight-binding molecular dynamics simulations using the environment-dependent tight-binding carbon potential. The nanodiamond is found to transform into a tube-shaped fullerene via annealing. Three interesting mechanisms for promoting inner carbon atoms of the nanodiamond into the surface carbon atoms of the tubular structure are observed. The “flow-out” mechanism prevails at temperatures lower than 2500 K and the “direct adsorption” and “push-out” mechanisms are observed at higher temperatures.

DOI: 10.1103/PhysRevLett.91.265701

PACS numbers: 64.70.Nd, 61.46.+w, 71.15.Pd, 81.05.Uw

Nanodiamond has attracted much interest since its first discovery in meteorites [1]. Several forms of nanometer-sized diamonds have been found in interstellar dusts [2], solid detonation products [3], and diamondlike films [4]. Recently, Raty *et al.* [5] performed *ab initio* calculations to study the structure of a nanodiamond with a diameter of  $\sim 1.4$  nm and found that the carbon nanoparticle consists of a diamond core and a reconstructed fullerenelike surface. While there are several experiments reporting that diamond nanoparticles of diameter  $\sim 5$  nm can be transformed into spherical and polyhedron carbon onions at high temperatures [6–8], the mechanism of such transformation is still not well understood. On the other hand, graphitization of the surface of bulk diamond has been an interesting subject of study for many years. From quantum molecular dynamics simulation studies of graphitization of the diamond (111) surface [9,10], it has been suggested that the formation of fullerenelike or graphitic surface structure appears to be one of the most effective ways of minimizing the surface-free energy at high temperatures. Here we attempt to probe the high temperature state of nanodiamonds, which is expected to provide a clue to the understanding of the formation as well as the growth mechanism of fullerenes, carbon nanotubes, and nanoclusters.

In this Letter, we present tight-binding molecular dynamics simulations on the structural transformation of nanodiamond at high temperature. The simulations show that upon annealing up to 2500 K the 1.4 nm-diameter nanodiamond is transformed into a fullerene structure with the shape resembling a single wall capped nanotube. During the course of the transformation, three mechanisms, namely, the “flow-out,” “direct adsorption,” and “push-out” mechanisms, are identified to play a crucial role in the conversion of the inner carbon atoms of the nanodiamond into the surface atoms of the tube-shaped fullerene. In particular, the flow-out mechanism is a

unique process in the transformation of a nanocluster to a fullerene structure, which is distinguished from other transformation mechanisms observed in diamond bulk surfaces.

The tight-binding molecular dynamics simulation is performed using the environment-dependent carbon tight-binding potential developed by Tang *et al.* [11]. This potential gives accurate energies for the various crystalline structures of carbon including diamond, graphite, linear chain, simple cubic, body-center cubic, and face-center cubic structures. The potential is also proven to describe well the surface reconstructions of diamond (111) and (100) surfaces, in addition to the vibration frequencies and elastic constants of diamond and graphite structures. The carbon tight-binding potential has been successfully applied to the simulation study of laser-induced structural transformation of the (111) surface of bulk diamond [10]. This tight-binding potential was also recently used to study the stability of carbon nanowire in the comparison with the stability of Si nanowire [12].

To start the simulation of nanodiamonds, we take a bulk-terminated carbon cluster of 275 atoms within a sphere of diameter of 1.4 nm cut from bulk diamond. This cluster is relaxed using the steepest descent method with the environment-dependent tight-binding carbon potential. The cluster structure after the relaxation is found to be similar to that of the previous *ab initio* generalized gradient approximation calculation [5]. Because of the surface reconstruction of nanodiamonds, there are graphitelike fragments present at the first atomic layer of the (111) facets, together with the formation of pentagons which link the graphene fragments to the underneath atoms [Fig. 1(a)]. The graphitelike fragments at the (111), ( $\bar{1}\bar{1}1$ ), ( $\bar{1}1\bar{1}$ ), and ( $1\bar{1}\bar{1}$ ) surfaces consist of three pentagons and three hexagons and those at the ( $\bar{1}11$ ), ( $1\bar{1}1$ ), ( $11\bar{1}$ ), and ( $\bar{1}\bar{1}\bar{1}$ ) surfaces consist of only

three pentagons. Starting from this relaxed cluster geometry, we perform tight-binding molecular dynamics simulation to investigate the structural transformation of the nanodiamond at high temperatures.

Figure 1 illustrates the snapshots of the atomic processes during the structural transformation of a nanodiamond into a tube-shaped fullerene through the simulations. First, the nanodiamond cluster was heated up to about 2500 K by constant-temperature molecular dynamics simulations. Near 2500 K, as shown in Fig. 1(b), the (111) surface layer of the nanodiamond begins to be graphitized after a simulation time of 3 ps; the exfoliation of the graphitized (111) layer occurs by breaking the bonds between graphene fragments and the underneath “core” atoms. This resembles the graphitization process of the (111) surface of bulk diamond induced

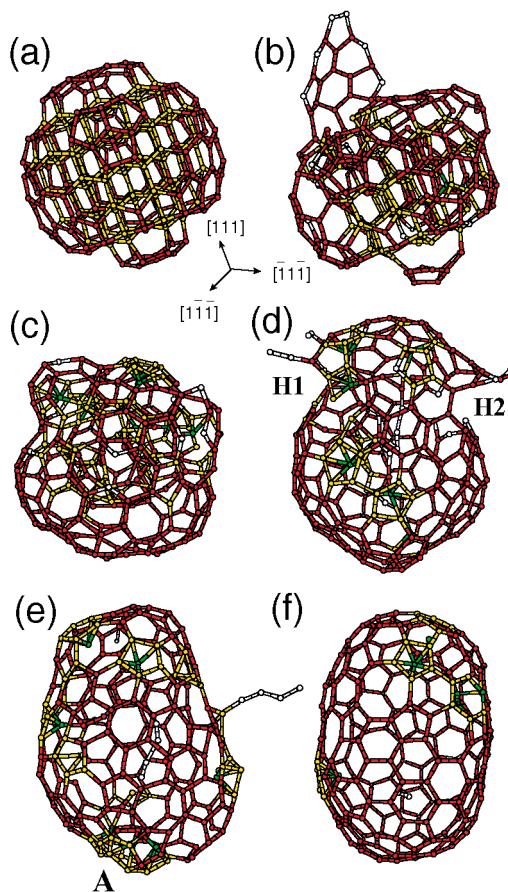


FIG. 1 (color). Atomic processes of structural transformation of nanodiamond to tube-shaped fullerene by successive annealings. (a) 0 K (at time  $t = 0$  ps), (b)  $\sim 2500$  K ( $t \approx 3$  ps), (c)  $\sim 2500$  K ( $t \approx 19$  ps), (d)  $\sim 2100$  K ( $t \approx 35$  ps), (e)  $\sim 1900$  K ( $t \approx 50$  ps), and (f)  $\sim 20$  K ( $t \approx 120$  ps). Simulated annealings with temperatures up to 3000 K are performed during the process (e)  $\rightarrow$  (f). The white color indicates atoms and bonds of two and less-fold coordination. Red and yellow colors indicate atoms and bonds of threefold coordination and fourfold coordination, respectively. Green colors indicate atoms and bonds of five and higher-fold coordination. Note that two holes H1 and H2 are created in (d). See the text for the part A in (e).

by nanosecond laser pulses [9,10]. As the simulation continues, the graphitized layer evaporates, breaking down into carbon dimers one by one from the end of the layer. Similarly, the  $(\bar{1}\bar{1}\bar{1})$  surface layer consisting of three pentagons undergoes the same exfoliation and evaporation process as that of the (111) surface. At about 18 ps, as shown in Fig. 1(c), the graphitization process becomes extended to the entire cluster surface. The core atoms and the surface “shell” atoms start to separate at the bottom side of the cluster. As the bonds between the core and shell atoms start to break up, the cluster begins to inflate similar to a bubble. At this stage, if the thermostat is maintained to keep the system at the constant temperature at 2500 K, the whole cluster would be completely evaporated within a simulation time of 45 ps. Thus, to prevent the full vaporization, we proceed to cool the system by decreasing the temperature from 2500 to 2000 K in 10 ps (during the simulation time between 25 and 35 ps). The cluster is then further cooled down to a temperature of  $\sim 1500$  K in 20 ps when a stable fullerene structure is found to form.

During these cooling processes, the number of threefold coordinated atoms increases remarkably while the number of fourfold coordinated atoms decreases. Contrary to the earlier heating-up stage in Fig. 1(b), where the graphitized layers are exfoliated and evaporated, the graphitized surface at this cooling-down stage evolves into a nanotube-wall shape. The two holes [“H1” and “H2” in Fig. 1(d)], as generated by the successive breaking of bonds among surface atoms, play an important role in pumping out the inner carbon atoms into the surface to form the graphitic layer, a process that we will refer to as the flow-out mechanism hereafter.

The flow-out mechanism operates during the cooling process from 2500 to 2000 K, which corresponds to the steps of Figs. 1(c)–1(e). Figure 2 shows in detail the flow-out process observed around the hole H1 on the top side of the cluster in Fig. 1(d). Before the holes open up, the inner atoms are confined by the surface atoms as shown in Fig. 2(a). Since the bonding between the inner and surface atoms consists of  $sp^3$ -type bonding, there still remain many fourfold coordinated atoms near the top side of the cluster [see also Fig. 1(c)]. As soon as the holes open up at the simulation time of  $\sim 22$  ps, the hole H1 becomes widely open as shown in Fig. 2(b). By breaking the  $sp^3$  bonds, the holes labeled as H1 and H2 in Fig. 1(d) are created on the top side of the cluster. During the simulation, the inner carbon atoms are pumped out into the surface through the holes, H1 and H2. Indeed these holes act as an “exit” for the inner atoms of the cluster. The inner atoms diffuse to the hole and flow out as shown in Fig. 2(c). Then, in Fig. 2(d), inner atoms are attached to surface atoms around the hole. As the diffusing inner atoms continue to flow through the hole [see Fig. 2(e)], the hole is fully plugged up and the tube-shaped fullerene is created as shown in Fig. 2(f).

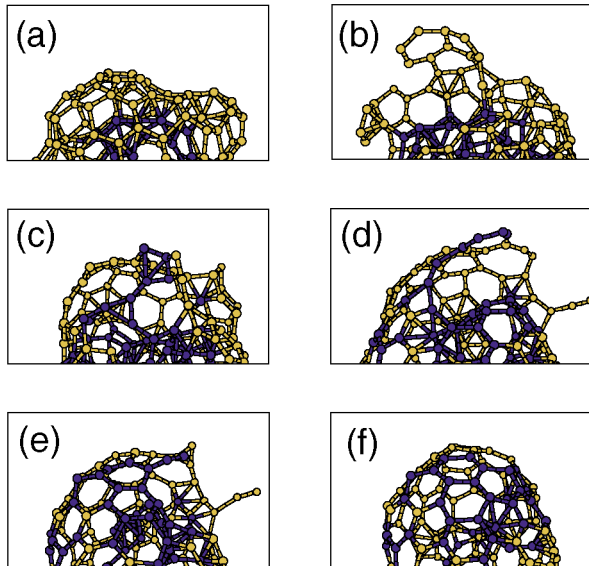


FIG. 2 (color). Flow-out mechanism observed around the hole H1 on the top side of the cluster labeled in Fig. 1(d). The process corresponds to the steps of Figs. 1(c)–1(e). (a)  $\sim 2500$  K ( $t \approx 19$  ps), (b)  $\sim 2600$  K ( $t \approx 24$  ps), (c)  $\sim 2500$  K ( $t \approx 25$  ps), (d)  $\sim 2100$  K ( $t \approx 33$  ps), (e)  $\sim 2000$  K ( $t \approx 45$  ps), and (f)  $\sim 1900$  K ( $t \approx 50$  ps).  $t$  is the total simulation time. The blue color indicates the inner atoms and bonds and the yellow color indicates the surface atoms and bonds at the starting configuration (a). The motion of blue atoms and bonds shows the process of promoting inner carbon atoms into surface carbon atoms.

When the incorporation of the inner carbon atoms into the tube wall around the holes is almost completed, we continue our MD simulation at the constant temperature 2000 K for another 10 ps. While the holes are being closed, the fullerene-like cage evolves into a shape close to capped nanotubes. However, as shown in Fig. 1(e), the fullerene-like cage still contains many defects such as linear chains, fourfold and fivefold coordinated atoms, and pentagon and heptagon rings. In order to reduce the number of defects, the cluster is again heated up to a temperature 3000 K in 4 ps and then is slowly cooled down. Through these annealing processes, the fullerene-like cage becomes a capped tube with a reduced number of defects as shown in Fig. 1(f). The tube-shaped cage structure, as obtained from the simulation, is consistent with the previous first-principles study which showed that, when the number of carbon atoms  $N > 240$ , the single-walled capped nanotube is energetically most stable among various forms of nanotubes and fullerenes [13].

During the annealing process, the operating mechanisms to incorporate the inner atoms into the surface atoms are different from the flow-out mechanism during the initial cooling process. Here two different mechanisms are found to be active: One is a direct adsorption mechanism and the other a push-out mechanism. As indicated by the green color in Fig. 1(e), those inner atoms that are directly attached to surface atoms are

very stable and persist even up to 2000 K  $\sim$  2500 K. When the temperature raises up to 3000 K in the annealing process, these atoms are observed to be changed to surface atoms by the direct adsorption or push-out mechanism.

Figure 3 illustrates the direct adsorption process, which corresponds to the evolution of part A marked in Fig. 1(e). At the beginning, four inner atoms (labels 1, 2, 3, and 4) are seen to adhere to the surface of the cage from inside. Atom 1 then moves to the center of a heptagonal ring [Fig. 3(b)], and breaks the bond at the boundary of the heptagonal and pentagonal ring [Fig. 3(c)]. It forms a  $sp^2$  bonding configuration as shown in Fig. 3(d). Atom 2 also breaks the bond at the boundary of the heptagonal and the other pentagonal ring [Fig. 3(d)]. Eventually, atoms 1 and 2 are combined and converted into surface atoms [Figs. 3(e) and 3(f)]. Consequently, by this direct adsorption process, the [pentagon-heptagon-pentagon] structure indicated by the yellow color in Fig. 3(a) transforms to the [hexagon-pentagon-hexagon] structure as shown in Fig. 3(f) and it contributes to the increase of the cage size.

Figure 4 illustrates the push-out process, which is observed in some part of the carbon cage in the steps of Figs. 1(e) and 1(f). In this mechanism, the inner carbon

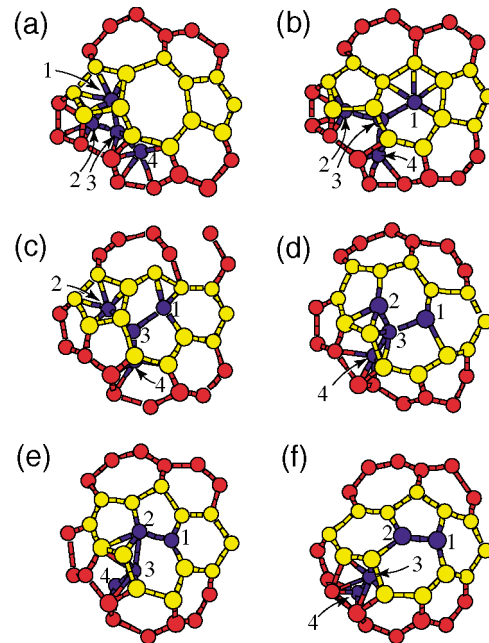


FIG. 3 (color). Conversion of inner carbon atoms into surface carbon atoms by the direct adsorption mechanism. (a)  $\sim 2500$  K ( $\Delta t = 0$  ps), (b)  $\sim 2900$  K ( $\Delta t = 0.31$  ps), (c)  $\sim 3000$  K ( $\Delta t = 1.29$  ps), (d)  $\sim 3000$  K ( $\Delta t = 1.46$  ps), (e)  $\sim 3000$  K ( $\Delta t = 1.54$  ps), (f)  $\sim 3000$  K ( $\Delta t = 1.84$  ps). (a) corresponds to the step of Fig. 1(e).  $\Delta t$  is the elapsed time relative to the moment of (a). The figure shows the part of the cluster marked by A in Fig. 1(e). Blue atoms indicate the inner atoms of the cluster at the moment of (a). Red and yellow atoms indicate surface atoms. See the text for a detailed description of the colors.

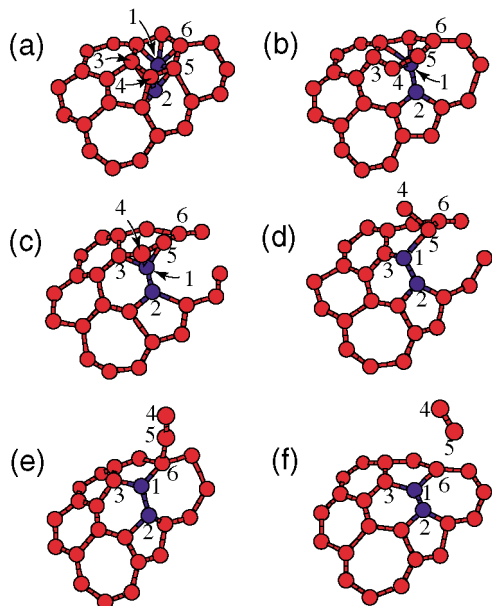


FIG. 4 (color). Conversion of inner carbon atoms into surface carbon atoms by the push-out mechanism. (a)  $\sim 2900$  K ( $\Delta t = 0$  ps), (b)  $\sim 2900$  K ( $\Delta t = 0.05$  ps), (c)  $\sim 2800$  K ( $\Delta t = 0.11$  ps), (d)  $\sim 2800$  K ( $\Delta t = 0.18$  ps), (e)  $\sim 2700$  K ( $\Delta t = 0.24$  ps), and (f)  $\sim 2700$  K ( $\Delta t = 0.32$  ps).  $\Delta t$  is the elapsed time relative to the moment of (a). The figure shows only a part of the cluster. Blue and red colors indicate inner and surface atoms, respectively, at the moment of (a).

atoms push the surface atoms into a vacuum and transform themselves into surface atoms. In Figs. 4(a) and 4(b) the inner atoms 1 and 2 are seen to move from one place to another, breaking their bonds with some surface atoms. A few moments later, surface atom 3 becomes a fourfold coordinated atom by bonding to the inner atom 1 [Fig. 4(c)], and then breaks the bond with atom 4 to keep its threefold coordination [Fig. 4(d)]. After the inner atom 1 forms a bond with atom 6, it breaks the bond with atom 5 [Figs. 4(d) and 4(e)]. Atom 6 also breaks the bond with atom 5 to keep its threefold coordination and the carbon dimer formed by atoms 4 and 5 is evaporated [Fig. 4(f)]. In this way, inner atoms 1 and 2 finally convert to surface atoms. Careful examinations of the simulation results reveal that the direct adsorption and push-out mechanism are induced by the nature of carbon atoms to keep the threefold coordination at high temperatures. As the temperature rises up to  $\sim 3000$  K, the fourfold coordinated inner atoms break their original  $sp^3$  bonds, migrate to the surface of the cluster, and incorporate into the wall of the tube-shaped fullerene in order to achieve the threefold coordinated configuration. This direct adsorption mechanism can contribute to the growth mechanisms of the nanotube as it plays a key role in increasing the size of the tube.

Recently, it was reported by experiment that a diamond nanoparticle of diameter  $\sim 5$  nm was transformed into

spherical carbon onions at  $\sim 2000$  K and into polyhedron carbon onions at  $\sim 2300$  K [7]. In the polyhedron carbon onions, the diameter of the smallest tube is approximately 1 nm, which is very similar to that ( $\sim 1.1$  nm) of the final geometry obtained from our simulation. Although the final geometry obtained from our present simulation as shown in Fig. 1(f) still contains some defects, we believe that, if the simulations can be performed for a sufficiently long time, a clean and perfect capped nanotube shall be obtained.

In summary, we have performed tight-binding molecular dynamics simulations to study the structural transformation of nanodiamond of diameter 1.4 nm, i.e., bucky diamond, by successive simulated annealing. In this simulation study, we observed the transformation of bucky diamond into a tube-shaped fullerene with the shape resembling a capped nanotube, and the diameter of the final structure is found to be very similar to that of the smallest tube inside the polyhedral carbon onion observed in experiments. Three kinds of mechanisms are found in the process of the conversion of the inner carbon atoms into the surface atoms of the tube. The transformation of bucky diamond into a tube-shaped fullerene is mostly dominated by the flow-out mechanism, while the other two mechanisms are observed to be effective during the higher temperature annealing process.

The authors are grateful to Dr. G. Galli for sending the preprint prior to publication [5]. This work was supported by the BK21 Program through the Ministry of Education, Korea. Ames Laboratory is operated for the U.S. Department of Energy by Iowa State University under Contract No. W-7405-Eng-82. This work was also supported by the Director for Energy Research, Office of Basic Energy Sciences, including a grant of computer time at the National Energy Research Supercomputing Center (NERSC) in Berkeley. J.Y. acknowledges the support by the KRF (Grant No. KRF-2000-015-DP0138) and by the MOST through the NSTP (Grant No. M1-0213-04-0001).

- 
- [1] R. S. Lewis *et al.*, *Nature (London)* **326**, 160 (1987).
  - [2] R. S. Lewis *et al.*, *Nature (London)* **339**, 117 (1989).
  - [3] N. R. Greiner *et al.*, *Nature (London)* **333**, 440 (1988).
  - [4] Y. K. Chang *et al.*, *Phys. Rev. Lett.* **82**, 5377 (1999).
  - [5] J. Y. Raty *et al.*, *Phys. Rev. Lett.* **90**, 037401 (2003).
  - [6] S. Tomita *et al.*, *Phys. Rev. B* **66**, 245424 (2002).
  - [7] S. Tomita *et al.*, *Chem. Phys. Lett.* **305**, 225 (1999).
  - [8] V. L. Kuznetsov *et al.*, *Chem. Phys. Lett.* **222**, 343 (1994).
  - [9] A. D. Vita *et al.*, *Nature (London)* **379**, 523 (1996).
  - [10] C. Z. Wang *et al.*, *Phys. Rev. Lett.* **85**, 4092 (2000).
  - [11] M. S. Tang *et al.*, *Phys. Rev. B* **53**, 979 (1996).
  - [12] Y. Zhao and B. I. Yakobson, *Phys. Rev. Lett.* **91**, 035501 (2003).
  - [13] N. Park *et al.*, *Phys. Rev. B* **65**, 121405(R) (2002).